On the Variability and Predictability of Eastern Pacific Tropical Cyclone Activity*

LOUIS-PHILIPPE CARON

Climate Forecasting Unit, Catalan Institute of Climate Sciences, Barcelona, Spain

MATHIEU BOUDREAULT

Department of Mathematics, Université du Québec à Montréal, Montréal, Québec, Canada

SUZANA J. CAMARGO

Lamont-Doherty Earth Observatory, Columbia University, Palisades, New York

(Manuscript received 21 May 2015, in final form 7 September 2015)

ABSTRACT

Variability in tropical cyclone activity in the eastern Pacific basin has been linked to a wide range of climate factors, yet the dominant factors driving this variability have yet to be identified. Using Poisson regressions and a track clustering method, the authors analyze and compare the climate influence on cyclone activity in this region. The authors show that local sea surface temperature and upper-ocean heat content as well as large-scale conditions in the northern Atlantic are the dominant influence in modulating eastern North Pacific tropical cyclone activity. The results also support previous findings suggesting that the influence of the Atlantic Ocean occurs through changes in dynamical conditions over the eastern Pacific. Using model selection algorithms, the authors then proceed to construct a statistical model of eastern Pacific tropical cyclone activity. The various model selection techniques used agree in selecting one predictor from the Atlantic (northern North Atlantic sea surface temperature) and one predictor from the Pacific (relative sea surface temperature) to represent the best possible model. Finally, we show that this simple model could have predicted the anomalously high level of activity observed in 2014.

1. Introduction

After years of below-average activity, 2014's eastern Pacific (EPAC) tropical cyclone (TC) season surged with one of the busiest seasons on record, with a total of 22 storms; 16 became hurricanes (HRs), and 9 of these were major hurricanes (MHRs). It was the most active year since 1992, the busiest season on record, and while most of these storms dissipated without affecting landmasses, there were notable exceptions, such as Hurricane Odile, which wreaked havoc in Cabo San Lucas in Baja California when it landed as a category 3 hurricane (down from category 4). As pointed out by Molinari and Vollaro (2000), the EPAC basin is the most active in terms of number of storms per unit area and unit time, and although a majority of these dissipate before making landfall, a nonnegligible number of TCs do impact the western coast of Mexico, either by hitting it directly or by brushing against the coast (Jáuregui 2003). In fact, besides being a catastrophic hazard, these TCs are also an important contributor of boreal summer precipitation for a large area of northwestern Mexico (Englehart and Douglas 2001) as well as the southwestern United States (Corbosiero et al. 2009; Ritchie et al. 2011; Wood and Ritchie 2013). (A complete list of acronyms used in this paper is given in Table A1.)

Unlike the Atlantic, where many of the climate factors modulating TC activity have been identified (Caron et al. 2015a), the factors modulating EPAC TC activity remain somewhat elusive. This makes it difficult to

* Supplemental information related to this paper is available at the Journals Online website: http://dx.doi.org/10.1175/JCLI-D-15-0377.s1.

Corresponding author address: Louis-Philippe Caron, Climate Forecasting Unit, Catalan Institute of Climate Sciences, Dr. Trueta 203, 3rd floor, Barcelona 08005, Spain.
E-mail: louis-philippe.caron@bsc.es

DOI: 10.1175/JCLI-D-15-0377.1

produce reliable seasonal forecasts of cyclone activity in this basin and, consequently, of rainfall for regions that derive a large part of their summer precipitation from these TCs. In effect, few groups produce TC forecasts for the region and even fewer make those forecasts widely available. One notable exception is the Climate Prediction Center (CPC), who (correctly) predicted above-average activity for 2014, based in part on expected El Niño conditions.

Camargo et al. (2007a) showed that El Niño–Southern Oscillation (ENSO) impacts potential intensity (a measure of the instability of the ocean–atmosphere system; Bister and Emanuel 1998) and vertical wind shear, two factors known to influence cyclogenesis, over the eastern North Pacific basin. More recently, Balaguru et al. (2013) and Jin et al. (2014) showed that EPAC TC activity was tied to local changes in upper-ocean heat content (UOHC), which they further linked to ENSO. In particular, Jin et al. (2014) showed that the heat accumulated during the boreal winter during El Niño events could be discharged a few months later in the region supporting cyclogenesis. Irwin and Davis (1999) further demonstrated that ENSO could shift the cyclogenesis location westward in that basin.

However, there is accumulating evidence that ENSO is not the prime modulator of TC activity in the EPAC basin despite its influence on some large-scale fields associated with cyclogenesis. While Gray and Sheaffer (1991) and Romero-Vadillo et al. (2007) found an increase in the number of intense hurricanes (categories 3–5) during El Niño events, Whitney and Hobgood (1997) found "little differences in the frequencies, maximum intensities, or relative intensities of TCs over the eastern North Pacific between El Niño and non–El Niño years." Collins and Mason (2000) later showed that while part of the cyclone variability in the western part of the EPAC could be explained by changes in the climatological environment with links to ENSO, cyclone variability in the eastern part could not, and because the number of cyclones forming in the eastern region (east of 116°W) is significantly larger than in the western part, ENSO could not explain basinwide variations in TC activity. Similar results were recently obtained by Jien et al. (2015) by dividing the basin into two regions at 112°W.

While the extent to which ENSO impacts EPAC TC activity has yet to be fully understood, the influence of El Niño on Atlantic tropical cyclone activity is fairly well documented (Klotzbach 2011; Kim et al. 2009; Camargo et al. 2007a; Landsea et al. 1999; Shapiro and Goldenberg 1998; Gray 1984) but is measured to be of the opposite sign as that suggested for the EPAC. In this case, the influence occurs mainly through changes in vertical wind shear, driven by changes in upper-level winds, over the Atlantic main development region (Goldenberg and Shapiro 1996). Changes in tropospheric humidity (Camargo et al. 2007a) and vertical stability (Tang and Neelin 2004) have also been implicated. This opposite reaction to ENSO could partly explain the significant anticorrelation in storm counts detected between the two basins (Frank and Young 2007; Collins 2010). However, ENSO cannot explain the slow variation observed in the EPAC hurricane record (Zhao and Chu 2006) or why this slow variation is also anticorrelated to hurricane activity in the Atlantic (Wang and Lee 2009). In fact, this slow variability makes the EPAC the only basin supporting TC activity with the peculiar feature of displaying a downward trend over the recent past (Kossin et al. 2007).

Wang and Lee (2009) linked this longer time-scale variability to changes in the Atlantic multidecadal oscillation (AMO), which has an opposite influence on cyclogenesis conditions in the EPAC compared to the North Atlantic; whereas in the Atlantic, a positive AMO phase is generally associated with lower wind shear conditions, Wang and Lee (2009) suggest that in the EPAC it is associated with higher wind shear as a result of anomalous upper-level easterly wind over part of the EPAC. Links between EPAC TC activity and vertical circulation over the tropical Atlantic were also noted by Zhang and Wang (2015), who found that an anticorrelation in the strength of the Hadley cells over the EPAC and the Atlantic, with associated change in vertical wind shear, could explain some of the observed anticorrelation.

Finally, besides the aforementioned climate factors, EPAC TC activity has also been linked to the slowly varying Pacific decadal oscillation (PDO; Martinez-Sanchez and Cavazos 2014; Lupo et al. 2008; Raga et al. 2013), to the North Atlantic Oscillation (NAO; Raga et al. 2013), and to the quasi-biennial oscillation (QBO; Whitney and Hobgood 1997), though this last relationship could not be reproduced in a more recent analysis (Camargo and Sobel 2010).

The goal of this paper is to compare the strength of the various climate influences that have been linked to EPAC cyclone activity and to determine the predominant climate factors that can explain the observed variability as well as those that ought to be considered in a seasonal forecast of EPAC TC activity. Section 2 describes the data used in this paper, section 3 gives a brief description of the Poisson regression used in this study, and results are presented in sections 4 and 5. An evaluation of our suggested seasonal forecast with out-of-sample data is presented in section 6, and a conclusion is given in section 7.

2. Data

a. Climate data

The choice of climate indices used in this study is based on previous literature discussing climate–cyclone interactions in the eastern Pacific. We first include a series of climate factors linked to the Pacific—namely, the ENSO, PDO, Pacific–North American pattern (PNA),[1] EPAC sea surface temperature (SST), and EPAC UOHC. Data for ENSO, PDO, and PNA are taken directly from the NOAA Earth System Research Laboratory (ESRL). The ENSO index is the bivariate ENSO time series calculated by combining the standardized Southern Oscillation index (SOI) and the standardized Niño-3.4 SST time series (Smith and Sardeshmukh 2000). The PDO (Zhang et al. 1997) is the leading principal component of monthly SST anomalies in the North Pacific Ocean, poleward of 20°N, while the PNA (Barnston and Livezey 1987) is the second leading empirical orthogonal function of Northern Hemisphere (20°–90°N) sea level pressure monthly anomaly covariance. EPAC SST is taken relative to the mean tropical SST (RSST), limited by 30°S and 30°N, and is taken as the average of NOAA extended reconstructed SSTs (ERSST; Smith et al. 2008) and Met Office Hadley Centre reconstructed SSTs (HadISST; Rayner et al. 2006) measured over 15°N, 30°N, 120°W, and 100°W. EPAC UOHC is derived from the EN4 dataset provided by the Met Office (Good et al. 2013) and is averaged over the same region as the EPAC SST over the first 110 m. Because the EPAC main development region is usually considered to start at around 8–10°N, we redid the entire analysis by extending the southern boundary of both EPAC SST and UOHC to 8°N. The results were not significantly impacted.

Because of the anticorrelation in TC activity observed between the Atlantic and the eastern Pacific, we also include a series of climate factors that have been linked to Atlantic TC activity—namely, the Atlantic meridional mode (AMM; Vimont and Kossin 2007; Kossin and Vimont 2007), AMO (Zhang and Delworth 2006; Knight et al. 2006), and NAO (Jagger et al. 2001; Elsner and Kocher 2000; Elsner et al. 2000), as well as western Sahel rainfall (Fink et al. 2010; Landsea and Gray 1992; Landsea et al. 1992), dust concentration over the tropical Atlantic (Evan et al. 2006, 2008), subpolar gyre (SPG) temperature (Smith et al. 2010; Dunstone et al. 2011), and tropical Atlantic SST (Vecchi et al. 2011; Swanson 2008; Camargo et al. 2013). The AMM (defined by Chiang and Vimont 2004), the AMO (linearly detrended SST averaged between 0° and 70°N), and the NAO (difference in pressures between Iceland and the Azores) are taken directly from the ESRL database. Sahel rainfall data come from the Joint Institute for the Study of the Atmosphere and Ocean (JISAO; Mitchell 2013), which uses Sahel averaging regions from Janowiak (1988) (10°N, 20°N, 20°W, 10°E). Dust concentration over the tropical Atlantic is derived from Evan and Mukhopadhyay (2010) and is averaged over 8°N, 20°N, 60°W, and 10°W. Atlantic SST is again measured with respect to the tropical mean and is the mean of ERSST and HadISST averaged over the region limited by 8°N, 20°N, 80°W, and 40°W, while the subpolar gyre temperature is measured over 50°N, 70°N, 60°W, and 20°W. Finally, we also include the QBO, given by the zonal winds at 30 hPa, which are provided by the University of Berlin (Naujokat 1986).

All of the climate indices are computed as the average for the July–September (JAS) period, the official hurricane season in the EPAC region, except for the western Sahel precipitation (June–September) and the NAO [both May–June (MJ) and JAS]. All data cover the period 1966–2013 except for the dust time series (1966–2008). Because of the unusual nature of the 2014 hurricane season with respect to the recent past, data for 2014 are not used in the analysis but will be used to evaluate our statistical seasonal forecast in a later section. The climate indices are shown in Fig. 1.

b. Hurricane data

Hurricane data are taken from the second-generation North Atlantic Hurricane Database (HURDAT2;[2] Landsea and Franklin 2013) maintained by the National Hurricane Center. Unlike the Atlantic basin where the TC record extends back to the end of the nineteenth century, data in the EPAC are more limited, beginning only in 1949. Even so, it is likely that a significant number of storms were missed prior to the satellite era and, despite some recent effort in that direction (Raga et al. 2013), there currently exists no solid estimation as to what that number might be. This stands in contrast to the Atlantic basin where such estimates are becoming available (Vecchi and Knutson 2008; Landsea et al. 2010; Vecchi and Knutson 2011; Chenoweth 2014). As such, we restrict our analysis to the satellite era and only consider hurricane data from 1966 onward. We construct annual time series for total number of cyclones,

[1] Although the PNA is not discussed in the TC literature, given its influence near the region of interest, we include it as a potential influence nonetheless.

[2] Downloaded on 4 June 2014.

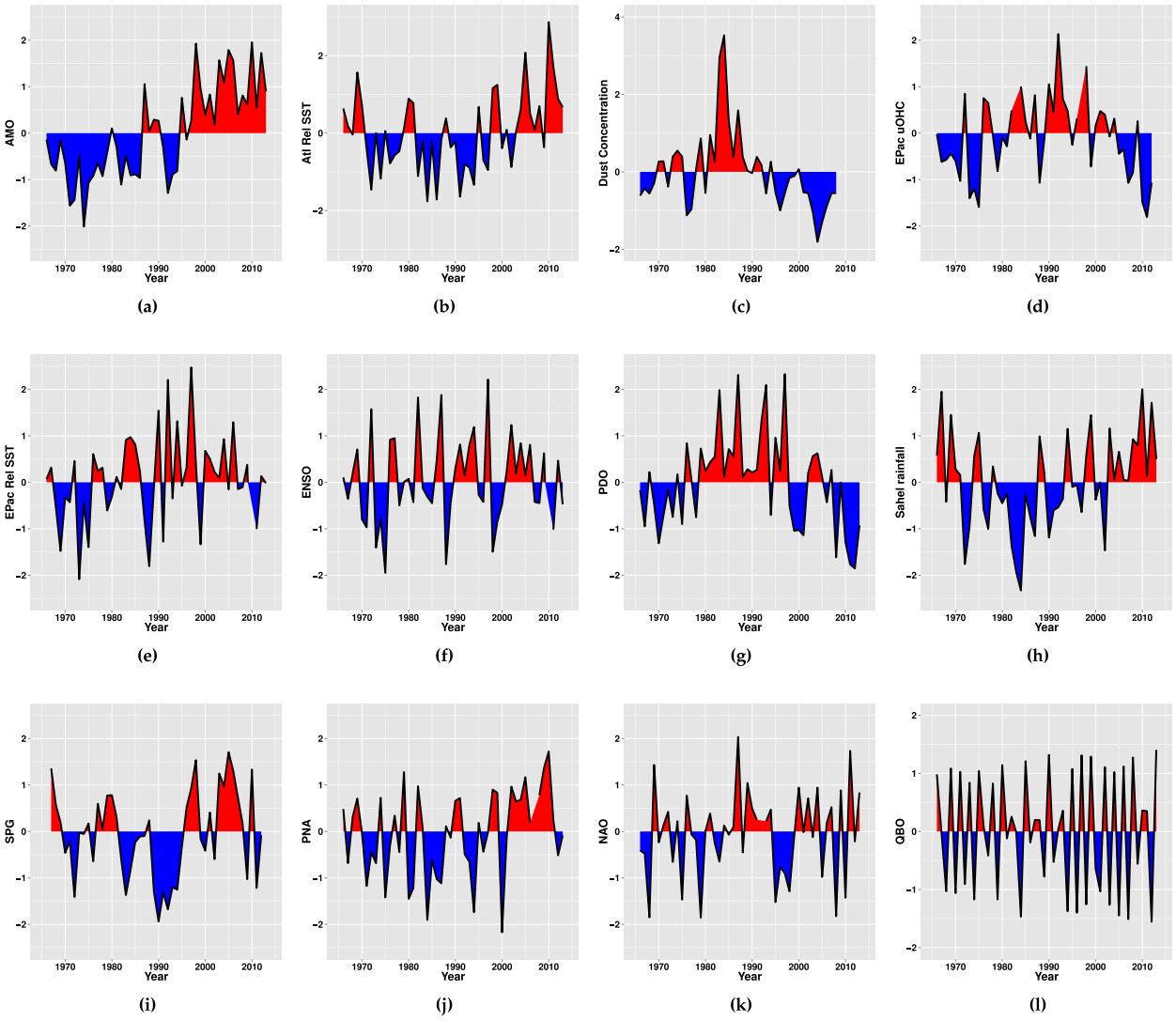

FIG. 1. Standardized time series of various climate indices used in this study: (a) AMO, (b) Atlantic (ATL) RSST, (c) dust concentration, (d) EPAC UOHC, (e) EPAC RSST, (f) ENSO, (g) PDO, (h) Sahel rainfall, (i) SPG temperature, (j) PNA, (k) NAO (MJ), and (l) QBO.

total number of cyclones that lasted 48 h or more [long-duration TCs (LTCs)], total number of hurricanes, and total number of major hurricanes (hurricanes of categories 3–5) using all storms present in the database of tropical storm intensity or higher. A time series of TCs with a lifetime of 48 h or more is included in order to address the artificial trend in short-duration storms present in the tropical cyclone record as a result of the constant improvement of satellite capabilities (Landsea et al. 2010). Each of the TC time series is shown in Fig. 2.

It was noted by Whitney and Hobgood (1997) that the EPAC hurricane data collected at the dawn of the satellite era (1966–70) are likely biased low in terms of intensity. As such, we redid the entire analysis using only data from 1971 onward. The significance of some of the weaker relationships (p values of ~5%) between hurricanes/major hurricanes and climate factors were impacted negatively (viz., PDO–HR, NAO–MHR, and PNA–MHR relationships). However, it had little impact on the relationships that were highly significant, the model selection analysis, and the skill of the hindcasts.

c. *Clustering*

The clustering method used here is based on a mixture of quadratic regression models, which are used to fit the geographical shape of tropical cyclone tracks. For each

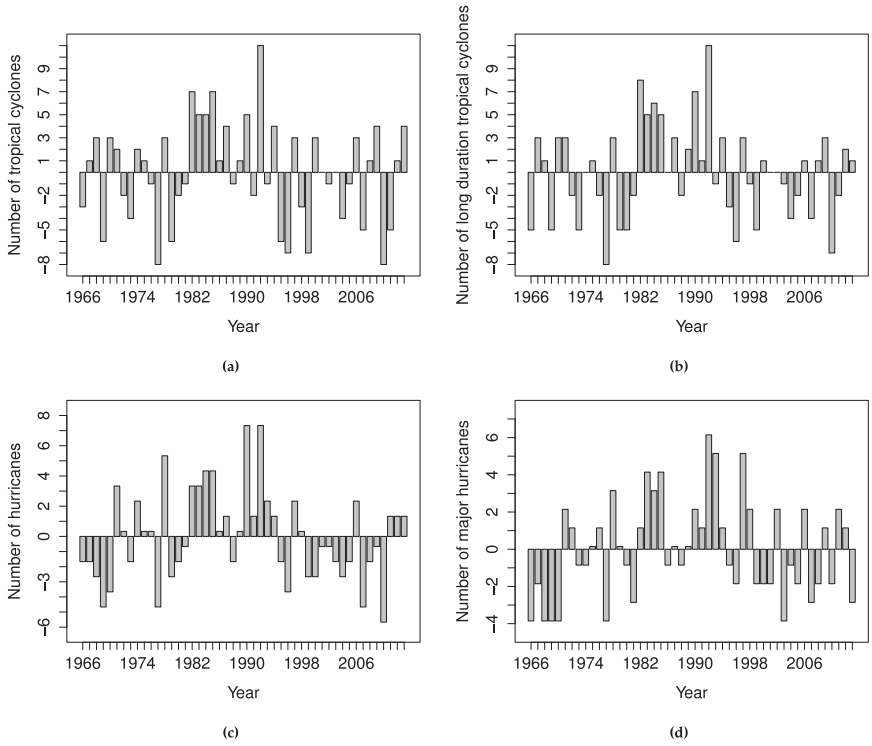

FIG. 2. Time series of EPAC (a) TCs, (b) TCs that lasted >48 h (LTCs), (c) HRs, and (d) MHRs for the period 1966–2013. The time series are expressed as anomalies with respect to the mean.

component (longitude and latitude), the mixture model uses a polynomial regression curve of storm position versus time. Each tropical cyclone track is then assigned to one of the K different regressions. Each model is defined by a set of different parameters, regression coefficients, and a noise matrix. Details of the technique are given in Gaffney et al. (2007), where it is applied to extratropical North Atlantic storms. This cluster technique has been widely applied to tropical cyclones in various regions—namely, in the western North Pacific (Camargo et al. 2007b,c), North Atlantic (Kossin et al. 2010), eastern North Pacific (Camargo et al. 2008), Southern Hemisphere (Ramsay et al. 2012), and Fiji region (Chand and Walsh 2009). More recently it was used to evaluate the similarity of model tracks to observations and to examine possible changes in model tracks in future climates (Daloz et al. 2015).

In Camargo et al. (2008) the technique was applied to all eastern North Pacific TCs of tropical storm intensity and higher for the period 1950–2006. Here, the analysis covers the period 1966–2013 and we not only consider all TCs but also examine the characteristics of the clusters for storms lasting 48 h or more and storms that have reached hurricane status. Clusters of major hurricanes only were excluded from this analysis because there were not a sufficiently large number of storms in the resulting time series to apply this particular methodology. Camargo et al. (2008) showed that the ideal number of clusters for describing TC activity in the EPAC region is three. Each of these clusters is shown in Fig. 3 (for the hurricane case) and Fig. S1 (for the TCs lasting $>$ 48 h), while Table 1 displays how many storms are contained in each cluster for each category of storms. It was also shown (Camargo et al. 2008) that the relationship with ENSO is significant in only one of the clusters (cluster 1), which includes the storms with significant westward shift in genesis and tracks compared to most of the TCs in the basin. The modulation of EPAC storms in intraseasonal time scales by the Madden–Julian oscillation (MJO) has also been well established (Maloney and Hartmann 2000) and was shown to be statistically significant for cluster 2.

3. Methodology

Analyses are based upon Poisson regressions, which is a common approach to model event counts in many contexts. The idea is to represent the mean of a Poisson distribution as a function of a set of predictors. When

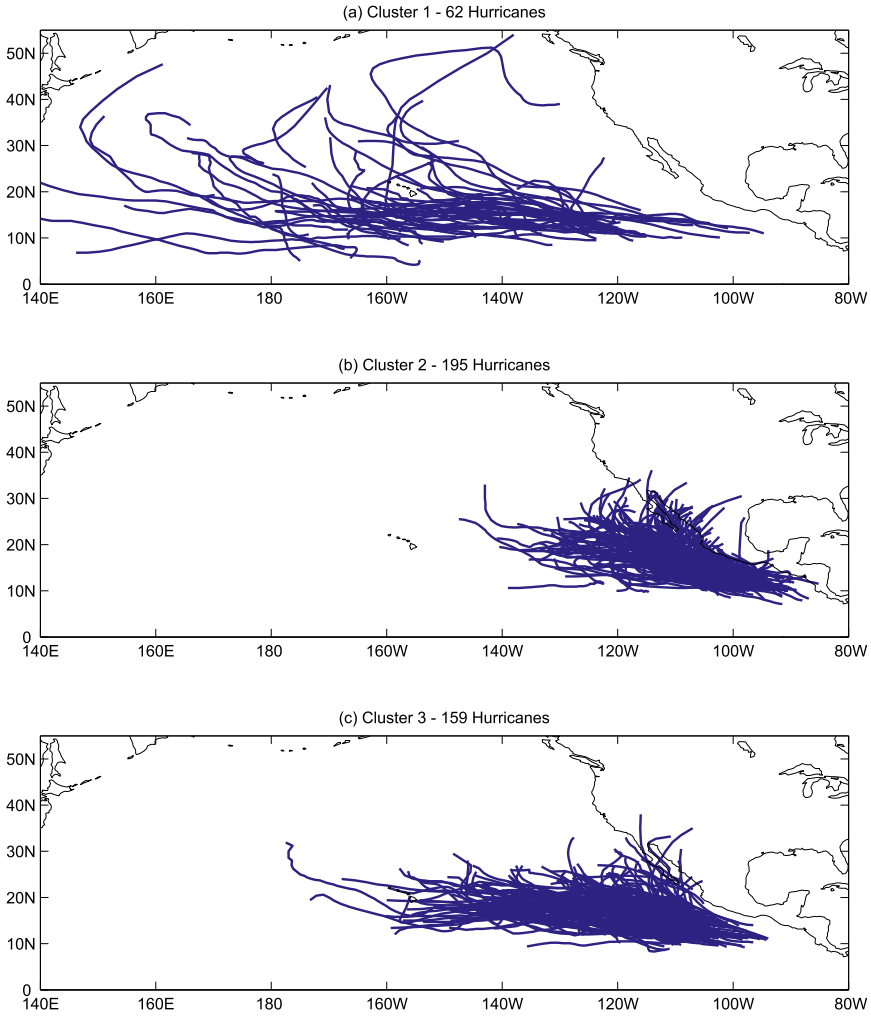

FIG. 3. The three clusters of eastern North Pacific hurricane tracks for the 1966–2013 period.

covariates are time varying, the mean is very often depicted as follows:

$$\lambda_k = \exp(\beta_0 + \beta_{1,k}X_{1,k} + \beta_{2,k}X_{2,k} + \cdots + \beta_{p,k}X_{p,k}), \quad (1)$$

where λ_k is the conditional mean (upon the predictors) of the Poisson distribution at time index k, $X_{j,k}$ is the value of the jth predictor at time k, and p is the total number of predictors in the model (excluding the constant β_0). Note that Eq. (1) is also known as the logarithmic link function since the log of the mean is linear in the predictors. In this case, $\beta_{j,k}$ is interpreted as the percentage change in λ_k when $X_{j,k}$ changes by one unit.

When investigating predictors of Atlantic TCs, the Poisson regression has been used by numerous authors: Solow and Nicholls (1990), Elsner (2003), Elsner and Jagger (2006), Villarini et al. (2010), Kozar et al. (2012), and Caron et al. (2015a), to name only a few. Poisson regressions have also been successfully used to construct genesis indices for global TC frequency and relate them to environmental variables in present and future climates (Tippett et al. 2011; Camargo et al. 2014). For an overview of the Poisson regression in climatology, one should refer to Elsner and Jagger (2013), and for a more general and comprehensive treatment of count regressions in statistics, we refer to Cameron and Trivedi (2013).

It has been shown by Gourieroux et al. (1984) that the value of $\beta_{j,k}$ is robust to model misspecification, meaning that the direction and size of the relationship does not depend on the underlying Poisson assumption. However, since we are largely interested in the significance of the relationships here, model misspecification may potentially affect some elements of the analysis. For this reason, we further validate the robustness of our results using Huber–White (sandwich) standard errors and negative binomial regressions. Finally, because the

TABLE 1. Number of storms per cluster for the 1966–2013 period.

	TCs	LTCs (>48 h)	HRs	MHRs
Cluster 1	125	98	62	33
Cluster 2	303	256	195	94
Cluster 3	340	270	159	58

number of observations in the eastern Pacific basin is rather small, bootstrapped p values are also computed. Overall, the focus will be on relationships that have very high significance (p values well below 5%) and that are also backed by solid geophysical explanations. Details of robustness analyses are provided in the supplementary material (Tables S1–S4).

4. Climate influence on eastern Pacific tropical cyclone activity

We summarize the results of the different Poisson regressions in Fig. 4, which shows to what extent, for each possible pair of predictand and predictor, a single covariate ($p = 1$) can help explain the number of storms basinwide or for a given cluster. This is done by examining the statistical significance of the predictor with its p value (bilateral test), which is computed with the maximum-likelihood estimates of a Poisson regression [Eq. (1)]. Red (blue) color represents a positive (negative) relationship between the predictor (climate factor) and the predictand (TC time series), whereas the tone of the color indicates the significance of the relationship (darker means more significant). Analyzing each possible pair makes the process prone to finding significant predictors by chance (multiple testing bias), further emphasizing the importance of focusing on relationships whose p values are well below 5%.

Initially concentrating on basinwide activity (i.e., TCs, LTCs, HRs, and MHRs), we see that the strongest predictors in the Atlantic are SPG(−), Atlantic RSST(−), and dust(+), as well as NAO (MJ)(+) and AMO(−), whereas in the Pacific, the best predictors are EPAC RSST(+), EPAC UOHC(+), and, to a lesser extent, PNA(−). A link between the PNA and typhoons in the western Pacific has already been established (Choi and Moon 2013), but to our knowledge, such a link has yet to

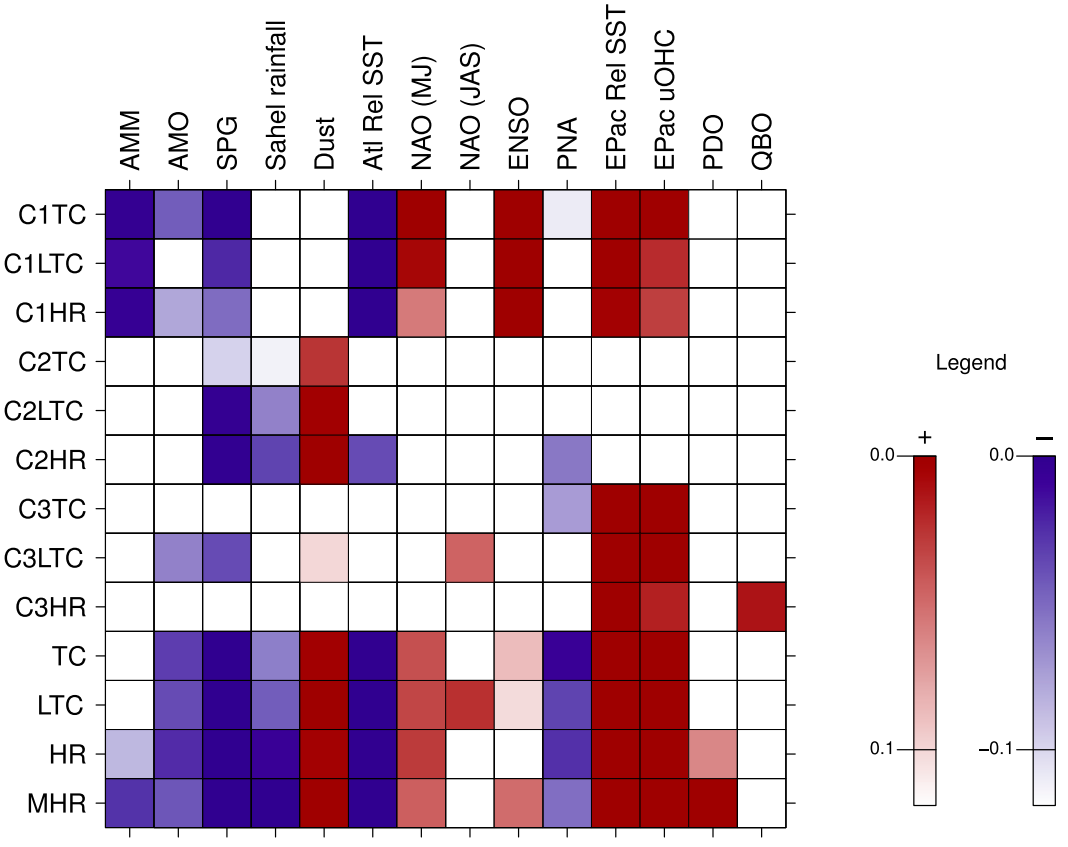

FIG. 4. Heat map showing p values of Poisson regressions for each pair of (left) predictand and (top) predictor. Blue (red) color refers to a negative (positive) relationship between the two (sign of the βs). Cx denotes cluster number x.

TABLE 2. Correlation between predictors. Values statistically significant at the 5% level are shown in bold.

	AMM	AMO	SPG	Sahel	Dust	ATL RSST	NAO (MJ)	NAO (JAS)	ENSO	PNA	EPAC RSST	EPAC UOHC	PDO	QBO
AMM	1.00	**0.76**	**0.36**	**0.49**	**−0.36**	**0.80**	−0.06	−0.13	−0.26	**0.32**	−0.09	−0.19	−0.18	0.17
AMO		1.00	**0.39**	**0.38**	**−0.35**	**0.66**	−0.11	**−0.34**	−0.09	**0.38**	−0.09	−0.15	−0.21	0.01
SPG			1.00	**0.49**	**−0.56**	**0.53**	**−0.31**	−0.23	−0.16	**0.28**	−0.15	**−0.45**	**−0.28**	0.07
Sahel				1.000	**−0.42**	**0.59**	−0.19	−0.21	**−0.44**	0.21	**−0.35**	**−0.46**	**−0.54**	0.00
Dust					1.00	**−0.31**	0.06	0.20	−0.19	**−0.37**	−0.04	**0.37**	0.19	−0.12
ATL RSST						1.00	−0.22	**−0.32**	**−0.48**	**0.35**	**−0.43**	**−0.42**	**−0.42**	0.20
NAO (MJ)							1.00	0.02	**0.33**	−0.19	0.24	0.20	0.14	0.06
NAO (JAS)								1.00	0.11	−0.01	0.19	0.17	0.17	0.07
ENSO									1.00	−0.02	**0.52**	**0.39**	**0.51**	−0.02
PNA										1.00	−0.21	−0.11	−0.01	−0.05
EPAC RSST											1.00	**0.53**	**0.34**	−0.07
EPAC UOHC												1.00	**0.63**	−0.07
PDO													1.00	0.05
QBO														1.00

be made for the EPAC. It is unclear at this time if there is a clear physical mechanism linking EPAC TC activity and the PNA or if this link is the result of the correlation between the PNA with other climate indices (Table 2). Interestingly, two climate indices local to the Pacific, ENSO and PDO, are significantly positive only when the strongest storms are considered (with p values of 4% and below 0.1%, respectively). Moreover, we have found no link at all between the QBO and any of the TC time series, in agreement with findings by Camargo and Sobel (2010) and Collins and Mason (2000). Finally, robustness analyses shown in Table S1 of the supplementary material further confirm the statistical significance of these relationships. The smaller number of observations for the dust time series implies that bootstrapped p values are adjusted upward, yet they still remain below 5%.

To better understand the respective impact of the Pacific and Atlantic variability on EPAC TC activity, we perform a similar analysis for each of the cluster time series (Fig. 4). Here, we detect large differences in the behavior of the three clusters. Cluster 1 is influenced both by factors from the Atlantic and the Pacific and is noticeably the only cluster significantly impacted by ENSO, as noted by Camargo et al. (2008). Since cluster 1 is composed mostly of storms forming in the western part of the basin, this result is also consistent with Collins (2010). On the other hand, cluster 3's variability seems largely tied to local thermodynamic conditions (more specifically, SSTs and UOHC), with only weak links to any other climate indices. This result supports the recent work of Jin et al. (2014), who showed that ocean heat content in the upper layer of the EPAC is important in modulating TC activity (as measured by accumulated cyclone energy) in that region (clusters 1 and 3 have on average the longest tracks and combined represent around 60% of all TCs). Strong ties between TC activity and thermodynamic factors in this region had also been noticed by Collins and Mason (2003).

Cluster 3 stands in contrast to cluster 2, which shows no particular Pacific influence and appears to be entirely modulated by the Atlantic basin, with statistically significant relationship to dust concentration, SPG temperature, Sahel precipitation, and Atlantic RSST. Interestingly, dust concentration is the predictor that returns the smallest p values among all the predictands (all below 0.5%). As previously mentioned, there exists a known link between the amount of precipitation over the Sahel region and the amount of dust over the tropical Atlantic (Wang et al. 2012), so it is not surprising to find a highly significant relationship for Sahel precipitation in this particular case.

Cluster 2 storms tend to form just off the coast of Central America, at the edge of the basin, suggesting that a large number of these storms have their origin in African easterly waves (AEWs), which have intensified upon reaching the EPAC owing to conditions generally favorable to cyclogenesis (Collins and Mason 2000). Poisson regressions between TC activity and the number of AEWs (derived from ERA-40; Uppala et al. 2005; S. Rowell and K. Hodges 2014, personal communication) crossing over to the Pacific during the EPAC hurricane season do not return significant p values for any of the cluster 2 predictands (not shown). The fact that there is no relationship between the absolute number of AEWs crossing into the Pacific and EPAC TC activity has been previously noted (Molinari and Vollaro 2000; Leppert et al. 2013).

To explain the influence of the Atlantic on cluster 2, we first note that the predictors local to the Atlantic basin that show the strongest link to the overall EPAC TC activity (SPG, Atlantic RSST, Sahel rainfall, dust

concentration, and AMO) are all correlated to some degree (see Table 2) and act in concert to modify large-scale fields by, for example, enhancing or inhibiting convective activity and TC formation over the Atlantic MDR (Wang et al. 2012; Klotzbach and Gray 2014; Dunstone et al. 2011). Using principal component (PC) analysis, we find that the proportion of variance explained by each of the five PCs of the Atlantic predictors is 57%, 17%, 14%, 8%, and 5%, respectively. Regressing each of the EPAC TC time series onto each of these PCs (Fig. 5), we find that only the first principal component is significantly linked (positively)[3] to changes in basinwide TC (and clusters 1 and 2) activity, suggesting that all the Atlantic predictors are capturing the same influence over EPAC TC activity.

Figure 6b shows the composite difference in JAS vertical wind shear (derived from NCEP reanalyses (Kalnay et al. 1996) for the 10 years with the highest (1984, 1972, 1983, 1982, 1974, 1991, 1986, 1992, 1971, and 1985) and lowest (2005, 1998, 2003, 2006, 2004, 1999, 2008, 1966, 1969, and 2007) first principal components. It shows that for years where the first principal component is high, seasonal vertical wind shear at the eastern edge of the North Pacific decreases; this reduction is collocated with the area where wind shear is maximum in a basin where wind shear conditions are generally favorable to cyclone formation (between 120° and 80°W in Fig. 6a). When a similar analysis is performed using other large-scale fields generally understood to influence cyclogenesis, none of them respond in such a way that could explain the observed change in EPAC TC activity (Fig. S2). Similarly, a regression of the first principal component onto vertical wind shear returns statistically significant negative relationships over most of the eastern North Pacific where TCs tend to form (Fig. S3a).

These results support those of Camargo et al. (2007a), who identified, using an entirely different approach based on genesis indices, changes in vertical wind shear as the main climate factor modulating EPAC TC activity. Furthermore, the results corroborate findings by Wang and Lee (2009) that vertical wind shear is the pathway through which the Atlantic influences EPAC TC activity.

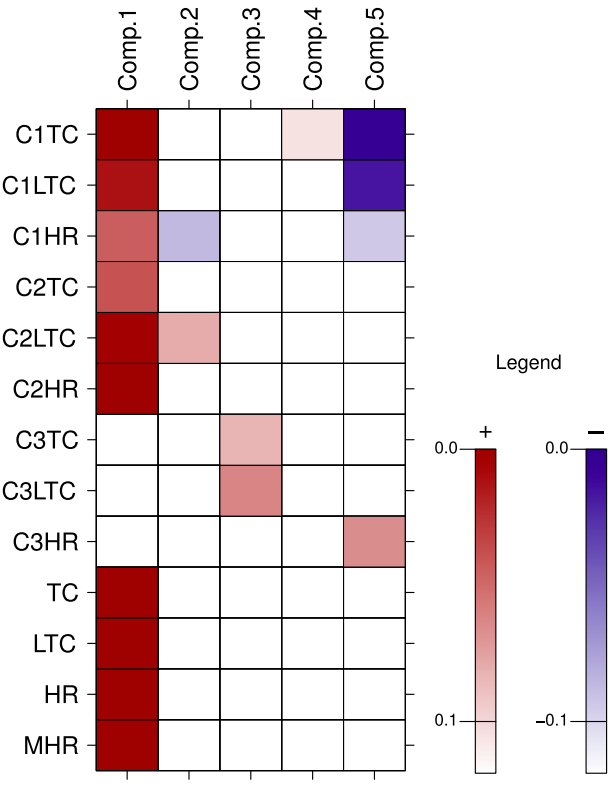

FIG. 5. Heat map showing p values of Poisson regressions for each pair of (left) predictand and (top) predictor (principal components). Blue (red) color refers to a negative (positive) relationship between the two (sign of the βs). The variance explained by each of the five principal components is 57%, 17%, 14%, 8%, and 5%, respectively. Tropical cyclones (TC), TCs that lasted >48 h (LTC), hurricanes (HR), major hurricanes (MHR), and cluster number x (Cx).

5. Model selection

a. Methods

The analysis of section 3 mainly focused on whether each variable, taken individually, had a link to EPAC TC frequency. This is a preliminary step in order to build a more complete model, one that may include one or several covariates. The goal of this section is to construct a model that has both an adequate in-sample fit and predictive power by combining the results of section 3 with model selection algorithms. Model selection algorithms look for predictors that optimize the in- or out-of-sample fit (as measured by the gain in log-likelihood or reduction in prediction errors) in comparison with the complexity of the model (as measured by the number of predictors in the model). For more details on model selection methods, we refer to James et al. (2013, chapters 5 and 6) and Hastie et al. (2009, chapters 3 and 7).

The best-known variable selection algorithm is the stepwise regression, with the forward method being the most popular. In a forward stepwise (Poisson) regression, the initial model is the Poisson distribution with constant mean, and each iteration seeks the predictor that adds the most to the log-likelihood. Variables are added until the gain in fit does not compensate the added complexity of

[3] A positive first principal component means less convective activity in the Atlantic.

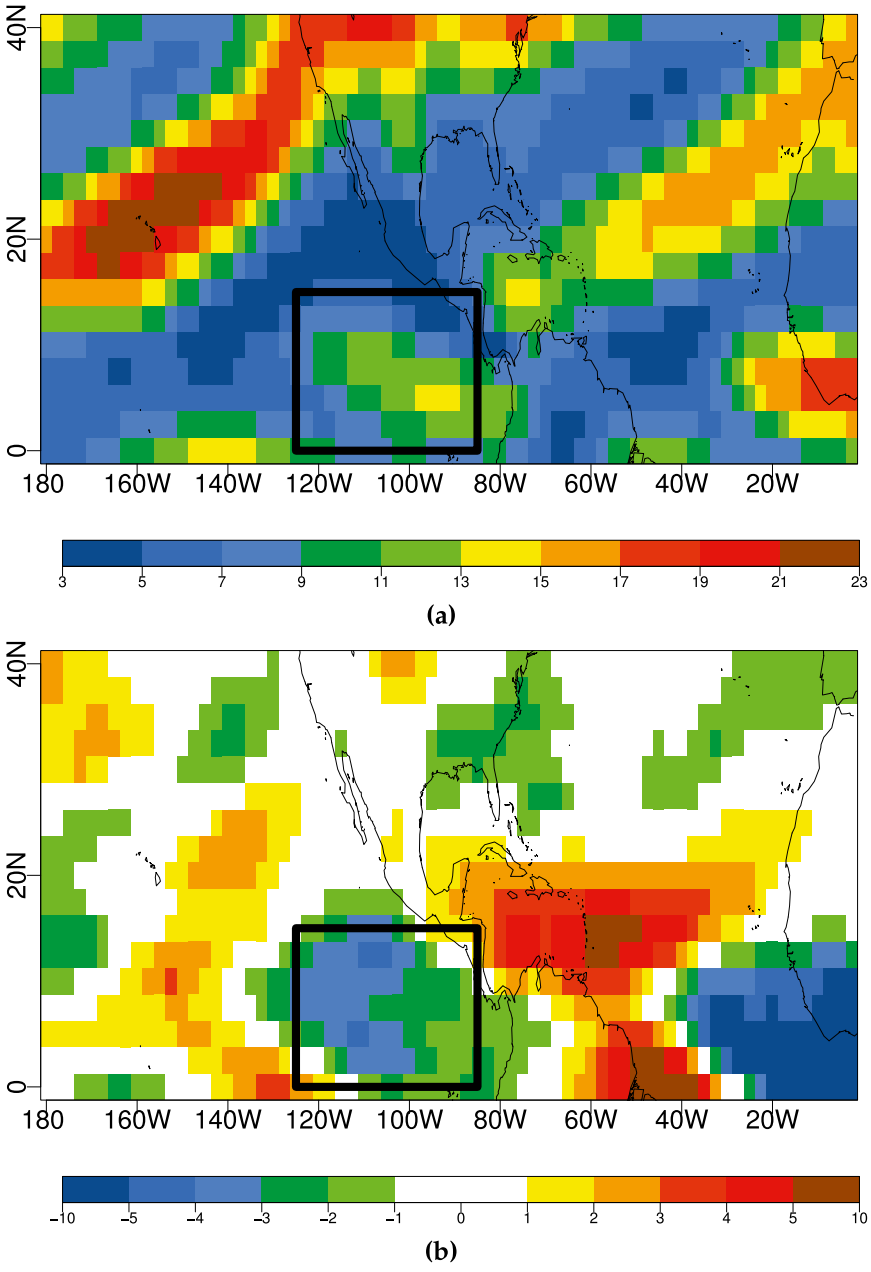

FIG. 6. (a) JAS climatology of vertical wind shear over the eastern Pacific. (b) Composite difference in vertical wind shear between the 10 years with the highest and lowest first principal component derived from the Atlantic predictors (AMO, Sahel rainfall, SPG, ATL RSST, and dust concentration). Years with a high first PC are 1984, 1972, 1983, 1982, 1974, 1991, 1986, 1992, 1971, and 1985. Years with a low first PC are 2005, 1998, 2003, 2006, 2004, 1999, 2008, 1966, 1969, and 2007. Years with a high (low) PC are associated with higher (lower) convective activity in the Atlantic. Vertical wind shear is measured between 850 and 200 hPa. Units: m s^{-1}.

the model. Information criteria such as the Akaike or Bayes information criteria (AIC or BIC) are generally used to weigh the gain in fit against the complexity of a statistical model. We note that the forward method has been applied in TC studies in the past by Kozar et al. (2012) and Villarini et al. (2010).

When the number of potential predictors is small, as is the case in this paper, another algorithm that can be used is one known as the best-subset selection. As the name suggests, it looks for the optimal combination of predictors among all possible cases. Optimality is usually defined on the basis of the quality of the in-sample fit

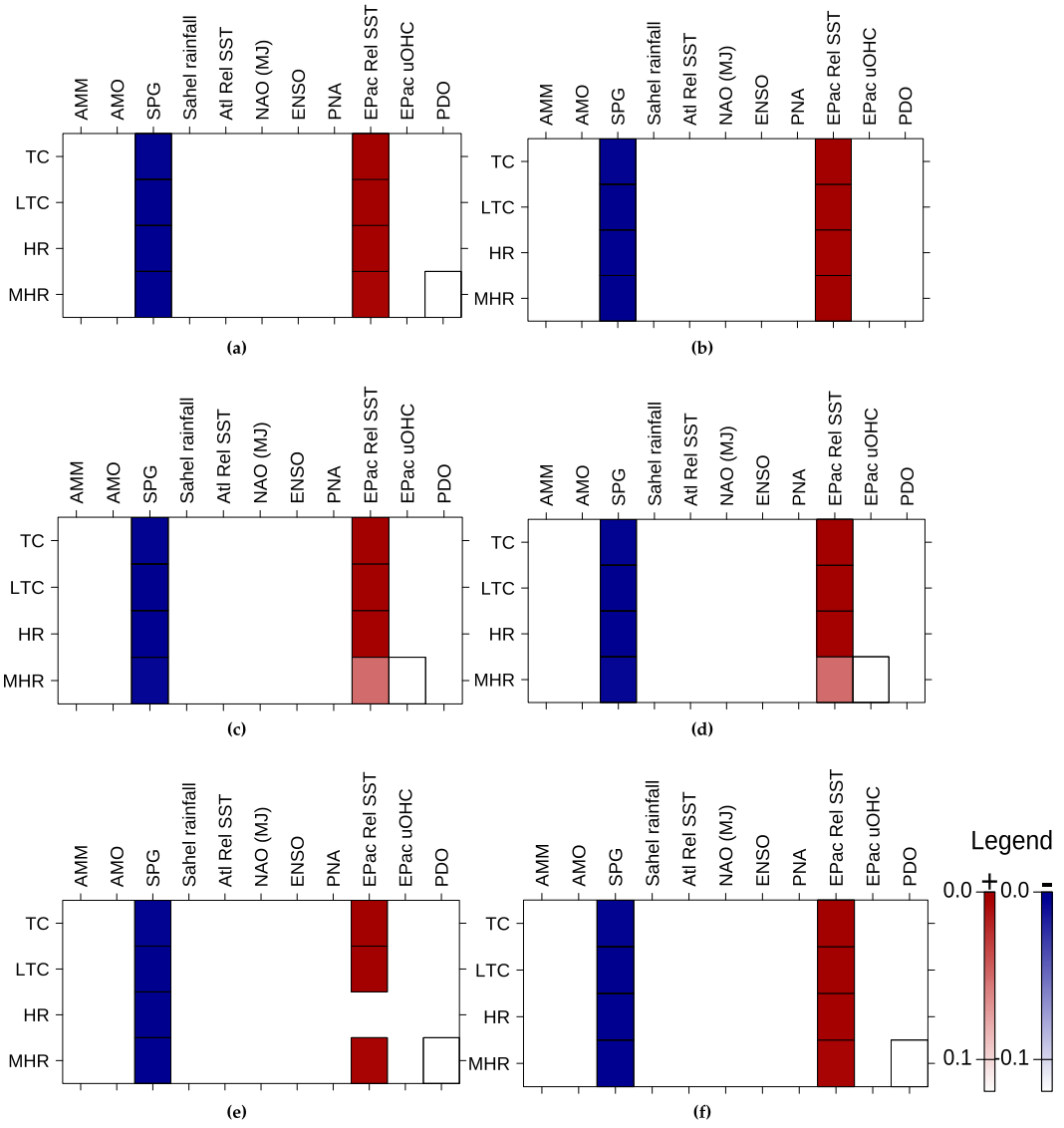

FIG. 7. Statistical models selected by the different selection algorithms: (a) bestglm (AIC), (b) bestglm (BIC), (c) forward selection (AIC), (d) forward selection (BIC), (e) fourfold CV, and (f) eightfold CV.

compared to the complexity of the model, as measured by an information criterion.

Stepwise and best-subset selection methods are not without issues. For example, as with multiple/simultaneous testing, there is a greater probability of finding a significant relationship by chance, resulting in underestimated p values. Another concern involves blindly using the output of the model regardless of its credibility. For a detailed account of issues related to automated model selection, we refer to Harrell (2001) and Burnham and Anderson (2002). It is important to note that a number of these issues are encountered and magnified in the field of data mining (machine/statistical learning), which is concerned with finding significant patterns within vast amounts of data. This is obviously not the case in our investigation, which is supported by geophysical explanations and supplementary statistical analyses.

Rather than looking at the quality of the in-sample fit, as with the stepwise and best-subset methods, one may instead consider the out-of-sample predictive capability of a model. One method tailored for this purpose is known as the k-fold cross-validation (CV) technique. The idea is to split the original sample into k random subsamples. Subsequently, one subsample is selected for validation while estimation is performed on the remaining data. The process is then repeated so that each subsample is used once for validation. The predictors are chosen to minimize

TABLE 3. The χ^2 GOF and likelihood ratio tests (LRTs) to assess the quality of in-sample fit of models chosen by selection algorithms.

χ^2 GOF test	Poisson	bestglm (BIC)	bestglm (AIC)	Forward (BIC)	Forward (AIC)	4-fold CV	8-fold CV
TC	0.1588	0.9167	0.9167	0.9167	0.9167	0.9167	0.9167
LTC	0.0891	0.9309	0.9309	0.9309	0.9309	0.9309	0.9309
HR	0.3779	0.9865	0.9865	0.9865	0.9865	0.8772	0.9865
MHR	0.0000	0.0088	0.0107	0.0104	0.0104	0.0107	0.0107
LRT	Poisson	bestglm (BIC)	bestglm (AIC)	Forward (BIC)	Forward (AIC)	4-fold CV	8-fold CV
TC	—	0.000 006	0.000 006	0.000 006	0.000 006	0.000 006	0.000 006
LTC	—	0.000 001	0.000 001	0.000 001	0.000 001	0.000 001	0.000 001
HR	—	0.000 012	0.000 012	0.000 012	0.000 012	0.000 163	0.000 012
MHR	—	0.000 000	0.000 000	0.000 000	0.000 000	0.000 000	0.000 000

the average prediction error for each of the subsamples. Note that CV has been used in Kozar et al. (2012) to assess the quality of each model; however, the *k*-fold CV technique was not applied to select the model itself.

Despite their drawbacks, selection algorithms can be useful for finding the most influential variables and can help provide guidance in model construction (McLeod and Xu 2014). In this section, we will use the forward, best-subset, and *k*-fold model selection techniques to help determine the best sets of predictors of TC frequency in the eastern Pacific basin. The step R function is used for the forward method, whereas the bestglm R package of McLeod and Xu (2014) is used for the second and third methods. To the authors' knowledge, the last two techniques have not previously been applied in TC studies.

b. *Best combinations of predictors*

As we are interested in forecasting the activity over the entire basin for the period covering 1966–2013, the analysis will be conducted on the total number of tropical cyclones, TCs lasting 48 h and longer, hurricanes, and major hurricanes. All three selection methods described in the previous subsection are applied to the latter four predictands. We exclude the QBO and NAO (JAS) as possible predictors based on the results of the previous section and the dust concentration since the latter does not cover the entire period of study.

Figure 7 illustrates which variables are chosen for each selection algorithm. The first row (Figs. 7a,b) corresponds to the best-subset technique, the second row (Figs. 7c,d) is the stepwise forward approach, and the last row (Figs. 7e,f) is the *k*-fold CV approach. For the first two rows, we applied both the AIC and BIC information criteria, whereas for the *k*-fold CV approach, both four and eight subsamples are used. As the original sample has 48 observations, each subsample consists of either 6 or 12 data points for validation purposes.

The two predictors that appear most often are the subpolar gyre and the EPAC relative SST. The relationship is positive for the EPAC relative SST and negative for the subpolar gyre temperature. This relationship holds true for almost all TC counts and methods. For major hurricanes, the subpolar gyre and the EPAC relative SST are clearly shown to be superior, yet a third predictor appears at times—either the PDO or the EPAC UOHC. The lack of statistical significance of this third predictor suggests that it should be discarded.

For a statistical model constructed using SPG and EPAC relative SST, we verified whether the significance of both predictors is affected by model misspecification or by the small sample size. With Huber–White (sandwich) standard errors, a negative binomial regression, or (nonparametric) bootstrap, both covariates remain highly significant. The complete results may be seen in Table S2 of the supplementary information.

We contend that a statistical model constructed using EPAC RSST and SPG temperature is relatively successful in capturing annual TC variability in the EPAC because it implicitly integrates both the local thermodynamic influence (significant for clusters 1 and 3) and the dynamical influence driven by the Atlantic (significant for clusters 1 and 2) known to influence cyclogenesis in that region. In the remaining portion of the paper, we will more thoroughly evaluate the skill with which this statistical model is able to predict TC activity over the EPAC basin.

c. *Goodness of fit*

To measure the ability of the subpolar gyre and the EPAC relative SST to form a complete model, Table 3 (top) shows the χ^2 goodness-of-fit (GOF) test for the resulting model of each selection method. It shows that a Poisson model with the latter two predictors is an adequate model for tropical cyclones, long duration TCs, and hurricanes. Note that even if the goodness-of-fit test cannot be rejected with a simple constant mean Poisson distribution, the *p* values are much smaller with the simple model, indicating that the in-sample fit is better when both predictors are added. The likelihood ratio

TABLE 4. Reduction (%) in the MSE compared to a simple Poisson distribution with constant mean. (top) Estimation over 1966–2009 and prediction over 2010–14; (bottom) estimation over 1966–2000 and prediction over 2001–14. MAE, MSEp, and MAEp are shown in Tables S3 and S4 in the supplementary information.

2010–14	ATL RSST + EPAC RSST	ATL RSST + EPAC UOHC	SPG + EPAC RSST	SPG + EPAC UOHC
TC	74.3	60.4	78.1	50.6
LTC	76.9	56.1	88.2	53.8
HR	44.9	30.4	65.2	37.2
MHR	21.9	8.3	37.1	13.9
2001–14	ATL RSST + EPAC RSST	ATL RSST + EPAC UOHC	SPG + EPAC RSST	SPG + EPAC UOHC
TC	52.1	31.8	58.9	27.9
LTC	56.4	34.7	72.8	35.6
HR	41.7	29.1	55.9	33.5
MHR	34.1	13.1	39.9	14.6

test (LRT), which is used to compare the quality of the in-sample fit of two nested models, also confirms the statistical significance of adding these two covariates (p values of the LRT are well below 0.1%) compared to a simple Poisson distribution. The LRT figures are shown in the bottom part of Table 3.

As for major hurricanes, the χ^2 goodness-of-fit test shows a p value of about 1% across techniques, meaning that despite the high significance of the covariates found, the lack of fit is important. One important reason for this lack of fit is the inability of the chosen models to capture the interannual variability of MHRs, as will be made clearer in section 6.

6. Out-of-sample hindcast

Section 5 showed that the SPG temperature and the EPAC RSST were the two most important predictors (among those considered) in trying to explain TC frequency in the eastern Pacific. In this section, we analyze the out-of-sample prediction capability of SPG and EPAC relative SST and compare it with four other plausible models.

The following five models are investigated: one simple Poisson distribution with constant mean and four Poisson regressions constructed using one variable from the Atlantic basin and one variable from the Pacific basin. In addition to SPG temperature and EPAC RSST, we include Atlantic RSST and EPAC OHC. The latter is closely tied to EPAC RSST, while the former is the most significant Atlantic predictor after SPG temperature (Fig. 4).

To assess the predictive capacity of a model, Elsner and Jagger (2013) suggest four different metrics. The mean absolute error (MAE) and the mean-square error (MSE) compute the sample mean of errors in absolute terms and in squared terms, respectively. The MAEp and MSEp measures are similar, but the error (either in absolute or squared terms) is weighted by the probability mass function of the underlying model. Therefore, the MAEp and MSEp also rely on the relevance of the distributional assumptions.

Each of the five models is fitted with data from 1966 to 2009. Using the observed values of the predictors between 2010 and 2014, it is possible to compute the mean number of events in each of these years and compare it with the realized number of storms. This is also known as an out-of-sample hindcast.

When building a statistical model in this context, we expect that the added complexity should yield better predictions than a simple Poisson distribution. Therefore, each entry in Tables 4, S3, and S4 corresponds to the relative reduction (in percent) in the forecast metric provided by a model compared with the same metric obtained with a simple Poisson distribution with constant mean. In Table 4 (top), we find that SPG temperature and EPAC RSST are the predictors that perform best for all predictands. The percentage reduction in the MSE is between 65% and 85% for TCs, LTCs, and hurricanes, whereas it is approximately 35% for major hurricanes.

A usual rule of thumb for validation exercises is that 70% of the sample is used for estimation (training), whereas 30% of the sample is used for forecast (validation). Therefore, we redo the same out-of-sample exercise, estimating the five models with data from 1966 to 2000, and perform predictions from 2001 to 2014. Table 4 (bottom) confirms the relevance of SPG and EPAC relative SST over the 14 predicted years. The other forecast metrics for both periods are shown in the supplementary information (Tables S3 and S4) with similar conclusions.

In Fig. 8, we illustrate the predictive performance of all five models over the years 2001–14. The bars correspond to the actual number of events in each year, whereas each line represents the predicted mean

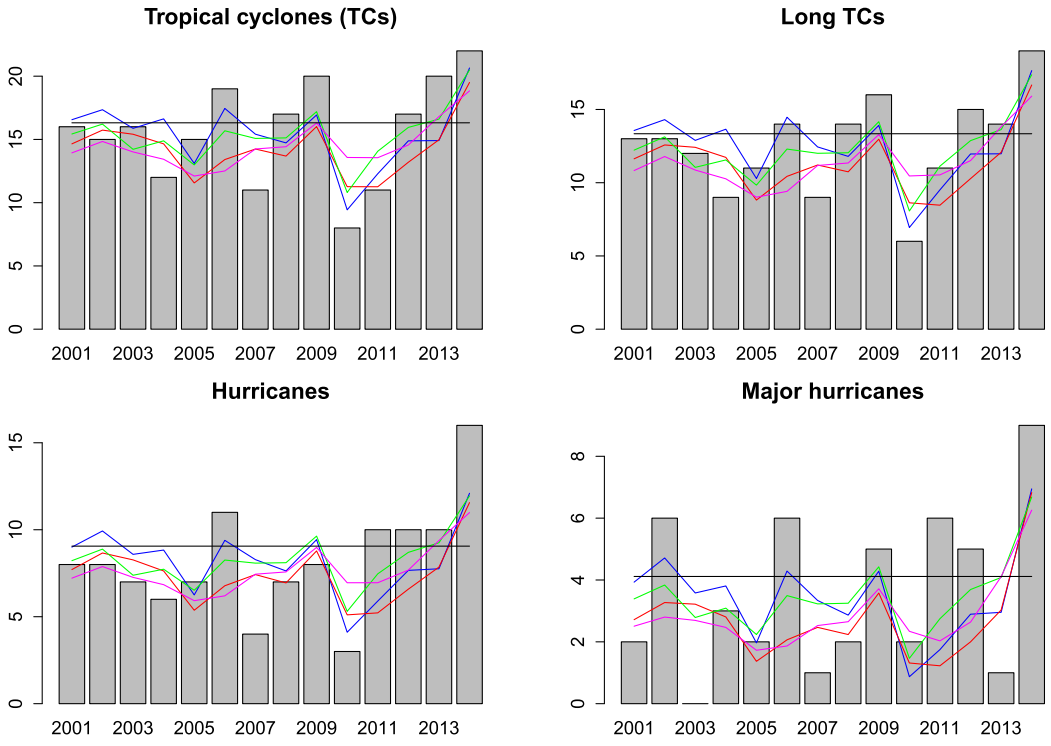

FIG. 8. Out-of-sample seasonal hindcasts for the 2001–14 period. Blue: ATL RSST + EPAC RSST. Red: ATL RSST + EPAC UOHC. Green: SPG + EPAC RSST. Magenta: SPG + EPAC UOHC.

provided by each of the four pairs of predictors. The figure shows that all four pairs of predictors appear to capture the decreasing pattern in 2001–04, the sudden increase in 2005–06, the drop in 2010, and the increasing trend in 2011–14. Note that these models would have predicted a very active season for 2014 (provided the SST had been accurately forecasted). As shown numerically in Table 4, the pair formed by SPG and EPAC relative SST (green line) provides the smallest forecast error. The exercise also illustrates why a constant mean assumption would likely fail in this situation.

It is important to note that according to Gourieroux et al. (1984), the estimation of the expected annual number of events λ_k is robust to model misspecification. This therefore indicates that the adequacy of the predicted means we calculated relies not on the Poissonian assumption but rather on the choice of the predictors.

Having a robust predicted mean is surely a desirable feature of a model, but as shown in Fig. 8, predicting interannual variability is also a very important feature. Figure 8 shows that the pairs of covariates perform very well in predicting the interannual variability in the number of TCs, LTCs, and hurricanes. The quality of the in-sample fit we obtained in section 5 and the robustness of the results to the various techniques both provided an important hint that these models would also do well out of sample.

As for major hurricanes, the predicted mean seems to be somewhat adequate, but the large interannual variability explains why the reductions in forecast metrics are much smaller. This further validates that we indeed found important covariates, but as both the in-sample fit and this exercise confirm, there is arguably something missing from the explanation of the interannual variability of major hurricanes.

In the presence of model uncertainty, as is the case with the choice of an appropriate pair of predictors in the EPAC, it is good practice to average the predicted mean over all four models. Model averaging is a well-known technique to help diminish model risk and improve predictions (Krishnamurti et al. 1999; Hastie et al. 2009). Figure 9 shows the evolution of the averaged predictions over the period 2001–14, in addition to the 2.5%, 25%, 75%, and 97.5% quantiles of a Poisson distribution with a mean given by this average. Actual observations of TCs, LTCs, and hurricanes fall most of the time within the 50% and 95% quantiles, but intervals tend to be very wide. As for major hurricanes, the year 2011 could be considered exceptional on the basis of the Poisson assumption; however, as previously discussed,

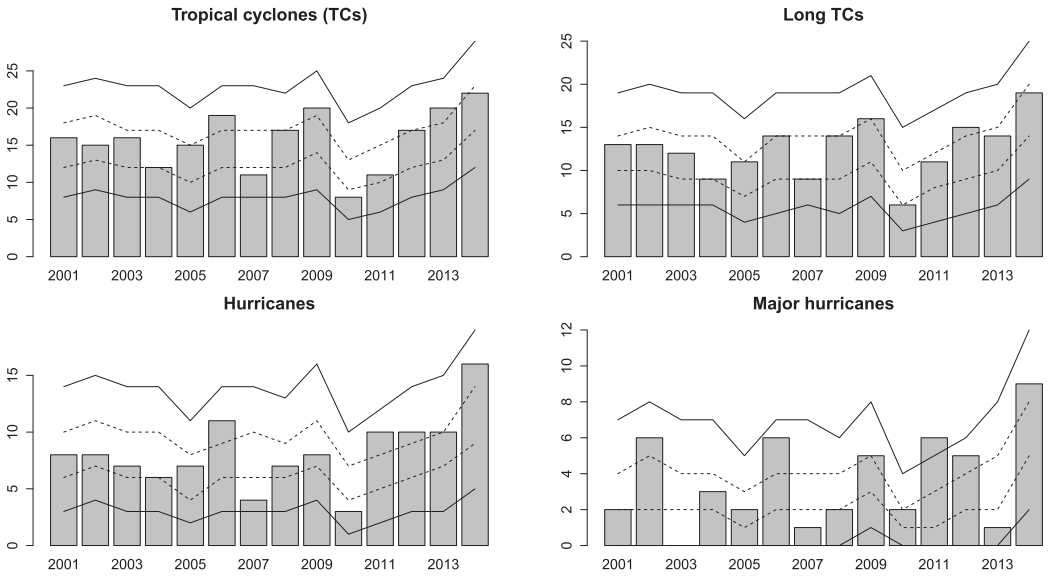

FIG. 9. Model-average out-of-sample seasonal hindcasts for the 2001–14 period with 50% (dash lines) and 95% (full lines) quantiles from a Poisson distribution.

the predictors fail to fully explain the interannual variability.

Overall, the forecast exercise shows that once the mean seasonal (JAS) temperature over the SPG and the EPAC regions have been predicted for a given year, it is then possible to determine with reasonable precision the level of TC activity in the EPAC basin for that same year. As shown in Figs. 8 and 9, these variables clearly help explain the anomalously high level of activity observed in 2014.

7. Concluding remarks

In this article, we have used Poisson regressions to compare the influence of different climate factors on modulating EPAC tropical cyclone activity over the recent past and to identify key factors that should be taken into consideration in a seasonal hurricane forecast for this particular region. The results confirm the importance of Atlantic large-scale conditions on EPAC TC variability and corroborate previous results suggesting that this influence occurs mainly through modulation of vertical wind shear over the EPAC basin. The Atlantic and EPAC basins thus appear as mirror images of each other in various ways; not only do the TCs anticorrelate owing to the opposite impact of many of the same influences, but also, wherein the Atlantic decadal variability is driven by changes in thermodynamic conditions (Emanuel et al. 2013), the EPAC decadal variability is driven by changes in dynamical conditions (resulting from the changes in Atlantic thermodynamic conditions).

Furthermore, using various model selection algorithms, we demonstrated that a reliable model of EPAC TC activity can be constructed using one predictor to account for the North Atlantic influence and another predictor to account for the conditions in the Pacific, with the best-performing model being the one that includes northern Atlantic SPG temperature and eastern Pacific RSST. This simple statistical model could even have anticipated the high level of activity of the 2014 hurricane season, provided the SST anomalies over these last two regions had been accurately forecasted. Interestingly, while SST forecasts in the Pacific region run into the ENSO predictability barrier, the northern North Atlantic is a region where initialized global climate models show a significant level of skill at predicting SSTs, even at the multiannual level (Doblas-Reyes et al. 2013; Kirtman et al. 2013; García-Serrano et al. 2015). This suggests that skillful predictions of TC activity in the EPAC, as in the Atlantic basin (Smith et al. 2010; Caron et al. 2014), might indeed be possible. In fact, much of the skill found in multiannual forecasts of Atlantic TC activity is derived from accurate predictions of SPG temperatures (Dunstone et al. 2011; Caron et al. 2015b).

Acknowledgments. The authors thank all the organizations and people who made their data available:

Amato Evan, Daniel Vimont, the National Hurricane Center, the NOAA Earth System Research Laboratory, the NOAA Climate Prediction Center, the Met Office Hadley Centre and the National Climatic Data Center, the Joint Institute for the Study of the Atmosphere and Ocean at the University of Washington, and the Department of Earth Sciences at the University of Berlin. A special thank you goes to Simon Rowell and Kevin Hodges for providing the AEW data. We are also grateful to Alexandre Cardin for helping develop the R code used to produce the heat maps, Katherine Barrett for proofreading this manuscript, and Francisco Doblas-Reyes and Neven Fučkar for sharing their insights. SJC acknowledges support from NSF Grant AGS 1143959 and NOAA Grant NA110AR4310093. MB acknowledges support from the Natural Sciences and Engineering Research Council of Canada. LPC acknowledges financial support from the EU-funded SPECS project (Grant 308378) and from the Ministerio de Economía y Competitividad (MINECO; Project CGL2014-55764-R). Finally, we are grateful to three anonymous reviewers for suggesting improvements to the original manuscript.

APPENDIX

Acronyms

TABLE A1. List of frequently used acronyms.

AEW	African easterly wave
AIC	Akaike information criteria
AMM	Atlantic meridional mode
AMO	Atlantic multidecadal oscillation
BIC	Bayes information criteria
CV	Cross validation
ENSO	El Niño–Southern Oscillation
EPAC	Eastern Pacific
GOF	Goodness of fit
HR	Hurricane
JAS	July–August–September
LRT	Likelihood ratio test
LTC	Long-duration (>48 h) tropical cyclone
MAE	Mean absolute error
MJ	May–June
MHR	Major hurricane
MSE	Mean-square error
NAO	North Atlantic Oscillation
PNA	Pacific North American pattern
PDO	Pacific decadal oscillation
QBO	Quasibiennial oscillation
RSST	Reconstructed sea surface temperature
SPG	Subpolar gyre
SST	Sea surface temperature
TC	Tropical cyclone
UOHC	Upper ocean heat content

REFERENCES

Balaguru, K., L. Ruby Leung, and J.-H. Yoon, 2013: Oceanic control of northeast Pacific hurricane activity at interannual timescales. *Environ. Res. Lett.*, **8**, 044009, doi:10.1088/1748-9326/8/4/044009.

Barnston, A. G., and R. E. Livezey, 1987: Classification, seasonality and persistence of low-frequency atmospheric circulation patterns. *Mon. Wea. Rev.*, **115**, 1083–1126, doi:10.1175/1520-0493(1987)115<1083:CSAPOL>2.0.CO;2.

Bister, M., and K. A. Emanuel, 1998: Dissipative heating and hurricane intensity. *Meteor. Atmos. Phys.*, **65**, 233–240, doi:10.1007/BF01030791.

Burnham, K., and D. Anderson, 2002: *Model Selection and Multimodel Inference*. Springer, 488 pp.

Camargo, S. J., and A. H. Sobel, 2010: Revisiting the influence of the quasi-biennial oscillation on tropical cyclone activity. *J. Climate*, **23**, 5810–5825, doi:10.1175/2010JCLI3575.1.

——, K. A. Emanuel, and A. H. Sobel, 2007a: Use of a genesis potential index to diagnose ENSO effects on tropical cyclone genesis. *J. Climate*, **20**, 4819–4834, doi:10.1175/JCLI4282.1.

——, A. W. Robertson, S. J. Gaffney, P. Smyth, and M. Ghil, 2007b: Cluster analysis of typhoon tracks. Part I: General properties. *J. Climate*, **20**, 3635–3653, doi:10.1175/JCLI4188.1.

——, ——, ——, ——, and ——, 2007c: Cluster analysis of typhoon tracks. Part II: Large-scale circulation and ENSO. *J. Climate*, **20**, 3654–3676, doi:10.1175/JCLI4203.1.

——, ——, A. G. Barnston, and M. Ghil, 2008: Clustering of eastern North Pacific tropical cyclone tracks: ENSO and MJO effects. *Geochem. Geophys. Geosyst.*, **9**, Q06V05, doi:10.1029/2007GC001861.

——, M. Ting, and Y. Kushnir, 2013: Influence of local and remote SST on North Atlantic tropical cyclone potential intensity. *Climate Dyn.*, **40**, 1515–1529, doi:10.1007/s00382-012-1536-4.

——, M. K. Tippett, A. H. Sobel, G. A. Vecchi, and M. Zhao, 2014: Testing the performance of tropical cyclone genesis indices in future climates using the HiRAM model. *J. Climate*, **27**, 9171–9196, doi:10.1175/JCLI-D-13-00505.1.

Cameron, A. C., and P. K. Trivedi, 2013: *Regression Analysis of Count Data Book*. Cambridge University Press, 566 pp.

Caron, L.-P., C. G. Jones, and F. Doblas-Reyes, 2014: Multi-year prediction skill of Atlantic hurricane activity in CMIP5 decadal hindcasts. *Climate Dyn.*, **42**, 2675–2690, doi:10.1007/s00382-013-1773-1.

——, M. Boudreault, and C. L. Bruyère, 2015a: Large-scale controls of Atlantic tropical cyclone activity with the phases of the Atlantic multidecadal oscillation. *Climate Dyn.*, **44**, 1801–1821, doi:10.1007/s00382-014-2186-5.

——, L. Hermanson, and F. Doblas-Reyes, 2015b: Multiannual forecasts of Atlantic U.S. tropical cyclone wind damage potential. *Geophys. Res. Lett.*, **42**, 2417–2425, doi:10.1002/2015GL063303.

Chand, S. S., and K. J. E. Walsh, 2009: Tropical cyclone activity in the Fiji region: Spatial patterns and relationship to large-scale circulation. *J. Climate*, **22**, 3877–3893, doi:10.1175/2009JCLI2880.1.

Chenoweth, M., 2014: A new compilation of North Atlantic tropical cyclones, 1851–98. *J. Climate*, **27**, 8674–8685, doi:10.1175/JCLI-D-13-00771.1.

Chiang, J. C., and D. J. Vimont, 2004: Analogous Pacific and Atlantic meridional modes of tropical atmosphere–ocean variability. *J. Climate*, **17**, 4143–4158, doi:10.1175/JCLI4953.1.

Choi, K.-S., and I.-J. Moon, 2013: Relationship between the frequency of tropical cyclones in Taiwan and the Pacific/North American pattern. *Dyn. Atmos. Oceans*, **63**, 131–141, doi:10.1016/j.dynatmoce.2013.05.003.

Collins, J., 2010: Contrasting high north-east Pacific tropical cyclone activity with low North Atlantic activity. *Southeast. Geogr.*, **50**, 83–98, doi:10.1353/sgo.0.0069.

——, and I. M. Mason, 2000: Local environmental conditions related to seasonal tropical cyclone activity in the northeast Pacific basin. *Geophys. Res. Lett.*, **27**, 3881–3884, doi:10.1029/2000GL011614.

——, and ——, 2003: Seasonal environmental conditions related to hurricane activity in the northeast Pacific basin. *N. Engl.–St. Lawrence Val. Geogr. Soc. Proc.*, **33**, 44–50.

Corbosiero, K. L., M. J. Dickinson, and L. F. Bosart, 2009: The contribution of eastern North Pacific tropical cyclones to the rainfall climatology of the southwest United States. *Mon. Wea. Rev.*, **137**, 2415–2435, doi:10.1175/2009MWR2768.1.

Daloz, A. S., and Coauthors, 2015: Cluster analysis of downscaled and explicitly simulated North Atlantic tropical cyclone tracks. *J. Climate*, **28**, 1333–1361, doi:10.1175/JCLI-D-13-00646.1.

Doblas-Reyes, F. J., and Coauthors, 2013: Initialized near-term regional climate change prediction. *Nat. Commun.*, **4**, 1715, doi:10.1038/ncomms2704.

Dunstone, N. J., D. M. Smith, and R. Eade, 2011: Multi-year predictability of the tropical Atlantic atmosphere driven by the high latitude North Atlantic Ocean. *Geophys. Res. Lett.*, **38**, L14701, doi:10.1029/2011GL047949.

Elsner, J. B., 2003: Tracking hurricanes. *Bull. Amer. Meteor. Soc.*, **84**, 353–356, doi:10.1175/BAMS-84-3-353.

——, and T. H. Jagger, 2006: Prediction models for annual U.S. hurricane counts. *J. Climate*, **19**, 2935–2952, doi:10.1175/JCLI3729.1.

——, and ——, 2013: *Hurricane Climatology: A Modern Statistical Guide Using R.* Oxford University Press, 390 pp.

——, and B. Kocher, 2000: Global tropical cyclone activity: A link to the North Atlantic Oscillation. *Geophys. Res. Lett.*, **27**, 129–132, doi:10.1029/1999GL010893.

——, K.-B. Liu, and B. Kocher, 2000: Spatial variations in major U.S. hurricane activity: Statistics and a physical mechanism. *J. Climate*, **13**, 2293–2305, doi:10.1175/1520-0442(2000)013<2293:SVIMUS>2.0.CO;2.

Emanuel, K. A., S. Solomon, D. Folini, S. Davis, and C. Cagnazzo, 2013: Influence of tropical tropopause layer cooling on Atlantic hurricane activity. *J. Climate*, **26**, 2288–2301, doi:10.1175/JCLI-D-12-00242.1.

Englehart, P. J., and A. V. Douglas, 2001: The role of eastern North Pacific tropical storms in the rainfall climatology of western Mexico. *Int. J. Climatol.*, **21**, 1357–1370, doi:10.1002/joc.637.

Evan, A. T., and S. Mukhopadhyay, 2010: African dust over the northern tropical Atlantic: 1955–2008. *J. Appl. Meteor. Climatol.*, **49**, 2213–2229, doi:10.1175/2010JAMC2485.1.

——, J. Dunion, J. A. Foley, A. K. Heidinger, and C. S. Velden, 2006: New evidence for a relationship between Atlantic tropical cyclone activity and African dust outbreaks. *Geophys. Res. Lett.*, **33**, L19813, doi:10.1029/2006GL026408.

——, and Coauthors, 2008: Ocean temperature forcing by aerosols across the Atlantic tropical cyclone development region. *Geochem. Geophys. Geosyst.*, **9**, Q05V04, doi:10.1029/2007GC001774.

Fink, A. H., J. M. Schrage, and S. Kotthaus, 2010: On the potential causes of the nonstationary correlations between West African precipitation and Atlantic hurricane activity. *J. Climate*, **23**, 5437–5456, doi:10.1175/2010JCLI3356.1.

Frank, W. M., and G. S. Young, 2007: The interannual variability of tropical cyclones. *Mon. Wea. Rev.*, **135**, 3587–3598, doi:10.1175/MWR3435.1.

Gaffney, S. J., A. W. Robertson, P. Smyth, S. J. Camargo, and M. Ghil, 2007: Probabilistic clustering of extratropical cyclones using regression mixture models. *Climate Dyn.*, **29**, 423–440, doi:10.1007/s00382-007-0235-z.

García-Serrano, J., V. Guemas, and F. J. Doblas-Reyes, 2015: Added-value from initialization in predictions of Atlantic multi-decadal variability. *Climate Dyn.*, **44**, 2539–2555, doi:10.1007/s00382-014-2370-7.

Goldenberg, S. B., and L. J. Shapiro, 1996: Physical mechanisms for the association of El Niño and West African rainfall with Atlantic major hurricane activity. *J. Climate*, **9**, 1169–1187, doi:10.1175/1520-0442(1996)009<1169:PMFTAO>2.0.CO;2.

Good, S. A., M. J. Martin, and N. A. Rayner, 2013: EN4: Quality controlled ocean temperature and salinity profiles and monthly objective analyses with uncertainty estimates. *J. Geophys. Res. Oceans*, **118**, 6704–6716, doi:10.1002/2013JC009067.

Gourieroux, C., A. Monfort, and A. Trognon, 1984: Pseudo maximum likelihood methods: Theory. *Econometrica*, **52**, 681–700, doi:10.2307/1913471.

Gray, W. M., 1984: Atlantic seasonal hurricane frequency. Part I: El Niño and 30 mb quasi-biennial oscillation influences. *Mon. Wea. Rev.*, **112**, 1649–1668, doi:10.1175/1520-0493(1984)112<1649:ASHFPI>2.0.CO;2.

——, and J. D. Sheaffer, 1991: El Niño and QBO influences on tropical cyclone activity. *Teleconnections Linking Worldwide Anomalies*, M. Glantz, R. Katz, and N. Nicholls, Eds., Cambridge University Press, 257–284.

Harrell, F., 2001: *Regression Modeling Strategies: With Applications to Linear Models, Logistic Regression, and Survival Analysis*. Springer, 572 pp.

Hastie, T., R. Tibshirani, and J. Friedman, 2009: *The Elements of Statistical Learning: Data Mining, Inference, and Prediction.* 2nd ed. Springer, 745 pp., doi:10.1007/978-0-387-84858-7.

Irwin, R. P., III, and R. E. Davis, 1999: The relationship between the Southern Oscillation index and tropical cyclone tracks in the eastern North Pacific. *Geophys. Res. Lett.*, **26**, 2251–2254, doi:10.1029/1999GL900533.

Jagger, T. H., J. B. Elsner, and X.-F. Niu, 2001: A dynamic probability model of hurricane winds in coastal counties of the United States. *J. Appl. Meteor.*, **40**, 853–863, doi:10.1175/1520-0450(2001)040<0853:ADPMOH>2.0.CO;2.

James, G., D. Witten, T. Hastie, and R. Tibshirani, 2013: *An Introduction to Statistical Learning: With Applications in R.* Springer, 426 pp., doi:10.1007/978-1-4614-7138-7.

Janowiak, J. E., 1988: An investigation of interannual rainfall variability in Africa. *J. Climate*, **1**, 240–255, doi:10.1175/1520-0442(1988)001<0240:AIOIRV>2.0.CO;2.

Jáuregui, E., 2003: Climatology of landfalling hurricanes and tropical storms in Mexico. *Atmósfera*, **16**, 193–204.

Jien, J. Y., W. A. Gough, and K. Butler, 2015: The influence of El Niño–Southern Oscillation on tropical cyclone activity in the eastern North Pacific basin. *J. Climate*, **28**, 2459–2474, doi:10.1175/JCLI-D-14-00248.1.

Jin, F.-F., J. Boucharel, and I.-I. Lin, 2014: Eastern Pacific tropical cyclones intensified by El Niño delivery of subsurface ocean heat. *Nature*, **516**, 82–85, doi:10.1038/nature13958.

Kalnay, E., and Coauthors, 1996: The NCEP/NCAR 40-Year Reanalysis Project. *Bull. Amer. Meteor. Soc.*, **77**, 437–471, doi:10.1175/1520-0477(1996)077<0437:TNYRP>2.0.CO;2.

Kim, H.-M., P. J. Webster, and J. A. Curry, 2009: Impact of shifting patterns of Pacific Ocean warming on North Atlantic tropical cyclones. *Science*, **325**, 77–80, doi:10.1126/science.1174062.

Kirtman, B., and Coauthors, 2013: Near-term climate change: Projections and predictability. *Climate Change 2013: The Physical Science Basis*, T. F. Stocker et al., Eds., Cambridge University Press, 953–1028, doi:10.1017/CBO9781107415324.023.

Klotzbach, P. J., 2011: El Niño–Southern Oscillation's impact on Atlantic basin hurricanes and U.S. landfalls. *J. Climate*, **24**, 1252–1263, doi:10.1175/2010JCLI3799.1.

——, and W. M. Gray, 2014: Qualitative discussion of Atlantic basin seasonal hurricane activity for 2015. Colorado State University Tech. Rep., 21 pp. [Available online at http://hurricane.atmos.colostate.edu/forecasts/2014/dec2014/dec2014.pdf.]

Knight, J. R., C. K. Folland, and A. A. Scaife, 2006: Climate impacts of the Atlantic multidecadal oscillation. *Geophys. Res. Lett.*, **33**, L17706, doi:10.1029/2006GL026242.

Kossin, J. P., and D. J. Vimont, 2007: A more general framework for understanding Atlantic hurricane variability and trends. *Bull. Amer. Meteor. Soc.*, **88**, 1767–1781, doi:10.1175/BAMS-88-11-1767.

——, K. R. Knapp, D. J. Vimont, R. J. Murnane, and B. A. Harper, 2007: A globally consistent reanalysis of hurricane variability and trends. *Geophys. Res. Lett.*, **34**, L04815, doi:10.1029/2006GL028836.

——, S. J. Camargo, and M. Sitkowski, 2010: Climate modulation of North Atlantic hurricane tracks. *J. Climate*, **23**, 3057–3076, doi:10.1175/2010JCLI3497.1.

Kozar, M. E., M. E. Mann, S. J. Camargo, J. P. Kossin, and J. L. Evans, 2012: Stratified statistical models of North Atlantic basin-wide and regional tropical cyclone counts. *J. Geophys. Res.*, **117**, D18103, doi:10.1029/2011JD017170.

Krishnamurti, T. N., C. M. Kishtawal, T. E. LaRow, D. R. Bachiochi, Z. Zhang, C. E. Williford, S. Gadgil, and S. Surendran, 1999: Improved weather and seasonal climate forecasts from multimodel superensemble. *Science*, **285**, 1548–1550, doi:10.1126/science.285.5433.1548.

Landsea, C. W., and W. M. Gray, 1992: The strong association between western Sahelian monsoon rainfall and intense Atlantic hurricanes. *J. Climate*, **5**, 435–453, doi:10.1175/1520-0442(1992)005<0435:TSABWS>2.0.CO;2.

——, and J. L. Franklin, 2013: Atlantic hurricane database uncertainty and presentation of a new database format. *Mon. Wea. Rev.*, **141**, 3576–3592, doi:10.1175/MWR-D-12-00254.1.

——, W. M. Gray, P. W. Mielke Jr., and K. J. Berry, 1992: Long-term variations of western Sahelian monsoon rainfall and intense U.S. landfalling hurricanes. *J. Climate*, **5**, 1528–1534, doi:10.1175/1520-0442(1992)005<1528:LTVOWS>2.0.CO;2.

——, R. A. Pielke Jr., A. M. Mestas-Nuñez, and J. A. Knaff, 1999: Atlantic basin hurricanes: Indices of climatic changes. *Climatic Change*, **42**, 89–129, doi:10.1023/A:1005416332322.

——, G. A. Vecchi, L. Bengtsson, and T. R. Knutson, 2010: Impact of duration thresholds on Atlantic tropical cyclone counts. *J. Climate*, **23**, 2508–2519, doi:10.1175/2009JCLI3034.1.

Leppert, K. D., D. J. Cecil, and W. A. Petersen, 2013: Relation between tropical easterly waves, convection, and tropical cyclogenesis: A Lagrangian perspective. *Mon. Wea. Rev.*, **141**, 2649–2668, doi:10.1175/MWR-D-12-00217.1.

Lupo, A. R., T. K. Latham, T. H. Magill, J. V. Clark, C. J. Melick, and P. S. Market, 2008: The interannual variability of hurricane activity in the Atlantic and east Pacific regions. *Natl. Wea. Dig.*, **32**, 119–135.

Maloney, E. D., and D. L. Hartmann, 2000: Modulation of eastern north Pacific Hurricanes by the Madden–Julian oscillation. *J. Climate*, **13**, 1451–1460, doi:10.1175/1520-0442(2000)013<1451:MOENPH>2.0.CO;2.

Martinez-Sanchez, J., and T. Cavazos, 2014: Eastern tropical Pacific hurricane variability and landfalls on Mexican coasts. *Climate Res.*, **58**, 221–234, doi:10.3354/cr01192.

McLeod, A., and C. Xu, 2014: bestglm: Best Subset GLM, version 0.34. R package. [Available online at http://cran.r-project.org/package=bestglm.]

Mitchell, T., 2013: Sahel precipitation index (20-10N, 20W-10E), 1900-October 2013. JISAO Climate Data Archive, accessed 14 May 2014, doi:10.6069/H5MW2F2Q.

Molinari, J., and D. Vollaro, 2000: Planetary- and synoptic-scale influences on eastern Pacific tropical cyclogenesis. *Mon. Wea. Rev.*, **128**, 3296–3307, doi:10.1175/1520-0493(2000)128<3296:PASSIO>2.0.CO;2.

Naujokat, B., 1986: An update of the observed quasi-biennial oscillation of the stratospheric winds over the tropics. *J. Atmos. Sci.*, **43**, 1873–1877, doi:10.1175/1520-0469(1986)043<1873:AUOTOQ>2.0.CO;2.

Raga, G. B., B. Bracamontes-Ceballos, L. M. Farfán, and R. Romero-Centeno, 2013: Landfalling tropical cyclones on the Pacific coast of Mexico: 1850-2010. *Atmósfera*, **26**, 209–220, doi:10.1016/S0187-6236(13)71072-5.

Ramsay, H. A., S. J. Camargo, and D. Kim, 2012: Cluster analysis of tropical cyclone tracks in the Southern Hemisphere. *Climate Dyn.*, **39**, 897–917, doi:10.1007/s00382-011-1225-8.

Rayner, N. A., P. Brohan, D. E. Parker, C. K. Folland, J. J. Kennedy, M. Vanicek, T. J. Ansell, and S. F. B. Tett, 2006: Improved analyses of changes and uncertainties in sea surface temperature measured in situ since the mid-nineteenth century: The HadSST2 dataset. *J. Climate*, **19**, 446–469, doi:10.1175/JCLI3637.1.

Ritchie, E. A., K. M. Wood, D. S. Gutzler, and S. R. White, 2011: The influence of eastern Pacific tropical cyclone remnants on the southwestern United States. *Mon. Wea. Rev.*, **139**, 192–210, doi:10.1175/2010MWR3389.1.

Romero-Vadillo, E., O. Zaytsev, and R. Morales-Pérez, 2007: Tropical cyclone statistics in the northeastern Pacific. *Atmósfera*, **20**, 197–213.

Shapiro, L. J., and S. B. Goldenberg, 1998: Atlantic sea surface temperatures and tropical cyclone formation. *J. Climate*, **11**, 578–590, doi:10.1175/1520-0442(1998)011<0578:ASSTAT>2.0.CO;2.

Smith, C. A., and P. Sardeshmukh, 2000: The effect of ENSO on the intraseasonal variance of surface temperature in winter. *Int. J. Climatol.*, **20**, 1543–1557.

Smith, D. M., R. Eade, N. J. Dunstone, D. Fereday, J. M. Murphy, H. Pohlmann, and A. A. Scaife, 2010: Skilful multi-year predictions of Atlantic hurricane frequency. *Nat. Geosci.*, **3**, 846–849, doi:10.1038/ngeo1004.

Smith, T. M., R. W. Reynolds, T. C. Peterson, and J. Lawrimore, 2008: Improvements to NOAA's historical merged land–ocean surface temperature analysis (1880–2006). *J. Climate*, **21**, 2283–2296, doi:10.1175/2007JCLI2100.1.

Solow, A., and N. Nicholls, 1990: The relationship between the Southern Oscillation and tropical cyclone frequency in the Australian region. *J. Climate*, **3**, 1097–1101, doi:10.1175/1520-0442(1990)003<1097:TRBTSO>2.0.CO;2.

Swanson, K. L., 2008: Nonlocality of Atlantic tropical cyclone intensities. *Geochem. Geophys. Geosyst.*, **9**, Q04V01, doi:10.1029/2007GC001844.

Tang, B., and J. Neelin, 2004: ENSO influence on Atlantic hurricanes via tropospheric warming. *Geophys. Res. Lett.*, **31**, L24204, doi:10.1029/2004GL021072.

Tippett, M. K., S. J. Camargo, and A. H. Sobel, 2011: A Poisson regression index for tropical cyclone genesis and the role of large-scale vorticity in genesis. *J. Climate*, **24**, 2335–2357, doi:10.1175/2010JCLI3811.1.

Uppala, S. M., and Coauthors, 2005: The ERA-40 Re-Analysis. *Quart. J. Roy. Meteor. Soc.*, **131**, 2961–3012, doi:10.1256/qj.04.176.

Vecchi, G. A., and T. R. Knutson, 2008: On estimates of historical North Atlantic tropical cyclone activity. *J. Climate*, **21**, 3580–3600, doi:10.1175/2008JCLI2178.1.

——, and ——, 2011: Estimating annual numbers of Atlantic hurricanes missing from the HURDAT database (1878–1965) using ship track density. *J. Climate*, **24**, 1736–1746, doi:10.1175/2010JCLI3810.1.

——, M. Zhao, H. Wang, G. Villarini, A. Rosati, A. Kumar, I. M. Held, and R. Gudgel, 2011: Statistical–dynamical predictions of seasonal North Atlantic hurricane activity. *Mon. Wea. Rev.*, **139**, 1070–1082, doi:10.1175/2010MWR3499.1.

Villarini, G., G. A. Vecchi, and J. A. Smith, 2010: Modeling the dependence of tropical storm counts in the North Atlantic basin on climate indices. *Mon. Wea. Rev.*, **138**, 2681–2705, doi:10.1175/2010MWR3315.1.

Vimont, D. J., and J. P. Kossin, 2007: The Atlantic meridional mode and hurricane activity. *Geophys. Res. Lett.*, **34**, L07709, doi:10.1029/2007GL029683.

Wang, C., and S.-K. Lee, 2009: Co-variability of tropical cyclones in the North Atlantic and the eastern North Pacific. *Geophys. Res. Lett.*, **36**, L24702, doi:10.1029/2009GL041469.

——, S. Dong, A. T. Evan, G. R. Foltz, and S.-K. Lee, 2012: Multidecadal covariability of North Atlantic sea surface temperature, African dust, Sahel rainfall, and Atlantic hurricanes. *J. Climate*, **25**, 5404–5415, doi:10.1175/JCLI-D-11-00413.1.

Whitney, L. D., and J. S. Hobgood, 1997: The relationship between sea surface temperatures and maximum intensities of tropical cyclones in the eastern North Pacific Ocean. *J. Climate*, **10**, 2921–2930, doi:10.1175/1520-0442(1997)010<2921:TRBSST>2.0.CO;2.

Wood, K. M., and E. A. Ritchie, 2013: An updated climatology of tropical cyclone impacts on the southwestern United States. *Mon. Wea. Rev.*, **141**, 4322–4336, doi:10.1175/MWR-D-13-00078.1.

Zhang, G., and Z. Wang, 2015: Interannual variability of tropical cyclone activity and regional Hadley circulation over the northeastern Pacific. *Geophys. Res. Lett.*, **42**, 2473–2481, doi:10.1002/2015GL063318.

Zhang, R., and T. L. Delworth, 2006: Impact of Atlantic multidecadal oscillations on India/Sahel rainfall and Atlantic hurricanes. *Geophys. Res. Lett.*, **33**, L17712, doi:10.1029/2006GL026267.

Zhang, Y., J. M. Wallace, and D. S. Battisti, 1997: ENSO-like interdecadal variability: 1900–93. *J. Climate*, **10**, 1004–1020, doi:10.1175/1520-0442(1997)010<1004:ELIV>2.0.CO;2.

Zhao, X., and P. S. Chu, 2006: Bayesian multiple changepoint analysis of hurricane activity in the eastern North Pacific: A Markov chain Monte Carlo approach. *J. Climate*, **19**, 564–578, doi:10.1175/JCLI3628.1.